Asymptotic breathing pulse in optical transmission systems with dispersion compensation

Ildar Gabitov
L. D. Landau Institute for Theoretical Physics, Kosygin Street 2, 117940 Moscow, Russia

Elena G. Shapiro
Institute of Automation and Electrometry, 630090 Novosibirsk, Russia

Sergei K. Turitsyn
Institut für Theoretische Physik I, Heinrich-Heine-Universität Düsseldorf, 40225 Düsseldorf, Germany
(Received 22 October 1996; revised manuscript received 5 December 1996)

We study a nonlinear process of the formation of a breathing solitary wave in the optical transmission systems with periodic amplification and dispersion compensation. Results of our numerical simulations demonstrate remarkably stable asymptotic propagation of such breathing pulse over long distances. We have derived approximate equations describing pulse amplitude and width oscillations and found that results obtained by this approach are in good agreement with the results of direct numerical modeling on the short and middle distances. It is shown that asymptotic averaged pulses have a form typically close to a Gaussian shape. We have found numerically that an input pulse evolves asymptotically into a stable breathing structure. After the first stage of propagation, the input pulse emits radiation that spreads due to dispersion. The asymptotic structure that is formed realizes a balance between the main pulse and the radiative tail. [S1063-651X(97)10203-3]

PACS number(s): 03.40.Kf, 42.65.Tg, 42.81.Dp

I. INTRODUCTION

One of the most important applications of the soliton theory is fiber optical communications. In order to satisfy the demands of future information transmission, which grows at an exponential rate, it is necessary to develop ultrafast optical transmission lines whose data transmission rates should eventually operate in a few hundred gigabits per second regime. The possibility of achieving such a goal was demonstrated in recent experiments [1–5]. Optical solitons are the real candidates to play the role of the carriers of information in such systems. Nonlinear models governing optical soliton transmission in fiber links are both of evident importance for applications and of a fundamental physical interest.

The problem of high-capacity system design falls into two categories: long-haul transmission systems based on low dispersion fibers (the zero dispersion point lies in the 1.55-μm window of optical transparency) and upgrading the existing fiber links based on standard telecommunication fibers (STFs). Recent progress in the fabrication of the erbium-doped fiber optical amplifiers operating at 1.55 μm and low dispersion fibers has already demonstrated the effectiveness of long-distance soliton-based optical communication systems (see, e.g., [2,6–8]). Lightwave transmission systems exploiting periodically distributed in-line optical amplifiers to compensate for a carrier pulse attenuation in the fiber will soon be installed as transoceanic communication links. The main feature of such a system is that amplifier spacing is considerably shorter than the characteristic dispersion length and therefore both the dispersion and nonlinearity can be treated as perturbations on the scale of the distance between amplifiers. Only the fiber losses and periodic amplification are significant factors in the leading order. These factors cause the amplitude oscillations, while the form of the pulse remains approximately unchanged. On a large scale pulse propagation in such communication systems is described by the well-established guiding-center (average) soliton theory [9,6,10]. The problem of upgrading the existing optical links, which are based on the standard telecommunication fiber, arise due to high (approximately 17 ps/nm km) dispersion in the 1.55-μm window of optical transparency. The optical amplifiers are usually placed at intervals of a few tens of kilometers for conventional transmission systems. The higher capacity of the transmission system requires shorter pulses. Therefore, the destructive influence of dispersion takes place at shorter distances. For multigigabit transmission at 1.55 μm the corresponding dispersion length in STFs is approximately equal to the amplification distance in the installed networks [11,12] and guiding-center soliton theory cannot be applied.

The influence of chromatic dispersion can be significantly reduced and the transmission capacity can be significantly enhanced by means of the dispersion compensation technique. The simplest optical-pulse equalizing system consists of a transmission fiber and a compensating fiber with the opposite dispersion [14]. The incorporation of a piece of fiber with high normal dispersion reduces the total dispersion of the fiber span between two amplifiers. Recent progress in the chirped fiber grating [13] allows dispersion of 500 ps/nm or even more to be compensated by a grating fiber a few decimeters in length. Presently the dispersion compensation is a simple and effective technique with many attractive features such as compatibility with the present concept of the all-optical transparency of the system, cascadability, and availability of all system components. The effectiveness of this method was demonstrated in several experiments [15–18] both for point-to-point and for cascaded transmission systems.

The soliton transmission using dispersion compensation fibers (DCFs) has recently become the focus of intensive research [19–30]. Large variations of the dispersion lead to the oscillations of a pulse width on the amplification distance. It was discovered in [23] that the resulting asymptotic pulse is close to the Gaussian shape and has energy well above that of the soliton of the average dispersion. Pulse dynamics in the nonlinear Schrödinger (NLS) equation with the dispersion varying as $d(z)=1+\epsilon\sin(kz)$ has been studied in [33,34] by means of the variational approach and numerically. It has been shown in [34] that while a very broad soliton is stable in such a model, the splitting of the fundamental soliton takes place if the modulation length is of the order of the dispersion length and the modulation amplitude exceeds a certain critical value. The dispersion-allocated soliton transmission line using dispersion-shifted nonsoliton fibers was suggested recently in [26]. In [28,21] the variational approach was used for the analysis of a pulse dynamics in optical communication systems with dispersion compensation. Modulation instability in the dispersion-managed optical lines was studied in [24–32]. Numerical simulations of the soliton transmission in short standard monomode fiber (SMF) systems upgraded by dispersion compensation have been performed in [12]. It has been shown that 10-Gbit/s transmission over 200 km is possible with a 36-km amplifier spacing. A theory of the average pulse propagation in systems using DCFs has been presented in [19]. It has been suggested to use breathing solitons for optical data transmission in STFs at 1.55 μm.

In this paper we study numerically and by means of the variational approach the asymptotic dynamics of the optical pulse in the transmission systems using the dispersion compensation technique. We have found that an asymptotically input signal evolves into the breathing soliton predicted in [19]. We derive an effective approximate model for pulse evolution by assuming that nonlinear effects and residual dispersion are responsible for ''slow'' average dynamics.

II. BASIC EQUATIONS AND VARIATIONAL APPROACH

The propagation of optical pulses in a transmission system with periodic amplification and dispersion compensation is governed by the (dimensionless) NLS equation

$$iA_z+\frac{Z_{\rm NL}}{2Z_{\rm dis}}d(z)A_{tt}+|A|^2A = iZ_{\rm NL}\left(-\gamma+[\exp(\gamma Z_a)-1]\sum_{k=1}^{N}\delta(z-z_k)\right)A = iG(z)A. \quad (1)$$

We use here the notation of [19]: $Z_{\rm NL}=1/\sigma P_0$ is the nonlinear length, $Z_{\rm dis}=t_0^2/|\beta_2|$ is the dispersion length corresponding to the STF (there are, as a matter of fact, three different dispersion lengths), t_0 and P_0 are the incident pulse width and peak power, β_2 is the group velocity dispersion for the STF, σ is the coefficient of the nonlinearity, γ describes fiber losses, Z_a is amplification period, and $z_k=kz_a$ are the amplifiers locations. Retarded time is normalized to the initial pulse width $t=T/t_0$, an envelope of the electric field $E=E(T,Z)$ is normalized to the initial pulse power $|E|^2=P_0|A|^2$, and the coordinate along the fiber z is normalized to the nonlinear length $z=Z/Z_{\rm NL}$. Chromatic dispersion $d(z)$ is normalized here to the STF dispersion coefficient.

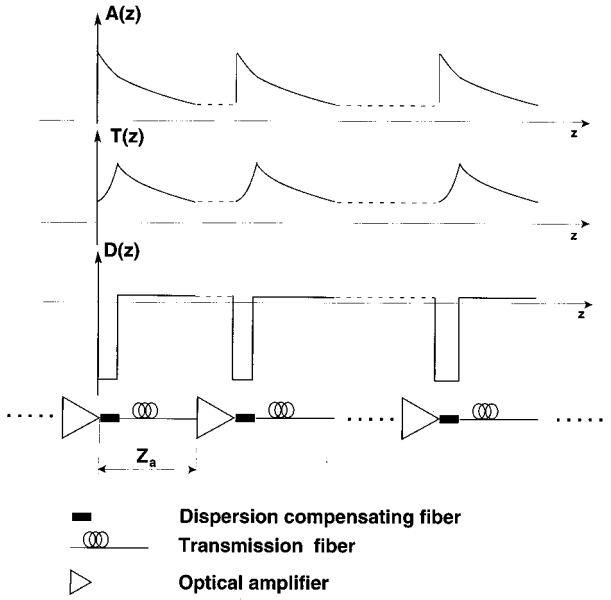

FIG. 1. Schematic diagram of the dispersion compensation. Dispersion compensating fibers are followed by pieces of transmission fibers. Dispersion $d(z)$ is normalized to the STF dispersion.

We consider without loss of generality the following dispersion-compensating scheme. A transmission line presents periodic alternating DCFs, transmission fiber sections, and in-line optical amplifiers as shown in Fig. 1. Each section includes a dispersion-compensated fiber with normal dispersion D_-, length Z_c, and segments of transmission fiber with anomalous dispersion D_+ and length $Z=Z_a-Z_c$. The average (residual) dispersion of the section is $D_{\rm res}=[D_-Z_c+D_+(Z_a-Z_c)]/Z_a$. To provide the average soliton propagation the residual dispersion $D_{\rm res}$ must be positive [19,12,26]. There are three characteristic dispersion scales in the system under consideration: a dispersion length $Z_{\rm DCF}$, corresponding to the chromatic dispersion of the DCF; a dispersion length of the transmission fiber $Z_{\rm dis}$; and a dispersion length that corresponds to the residual dispersion of each section $Z_{\rm RD}$. An optical pulse propagating in such a system experiences periodic oscillations of the amplitude and width. A pulse evolution in the transmission line in the first approximation can be described as a quasilinear process. In the first stage, pulses acquire a positive dispersion-induced frequency chirp induced by a DCF. The pulse width increases in this stage due to dispersive broadening. Entering a piece of a STF pulses compress because the sign of the dispersion is reversed and the condition for dispersion-induced compression $\beta_2C<0$ is satisfied (see, e.g., [35]). During propagation in fibers the amplitude of the pulse is reduced due to fiber losses. Therefore, pulses must be regenerated at the end of each section. In cascaded systems such a basic section including a DCF, a STF, and an optical amplifier is periodically repeated. When nonlinear effects and residual dispersion are negligible the pulse recovers its original form. Indeed, a phase shift of the pulse corresponding to the Kerr effect over one cycle of this process is small; therefore,

dispersion and fiber losses are the main acting factors. However, these small changes are collected and at larger distances the Kerr nonlinearity may begin to come into play. The influence of residual dispersion appears at a distance of $Z_{\mathrm{RD}} \gg Z_a$ and alters the shapes of pulses. The nonlinear length Z_{NL} can be comparable with Z_{RD}. Therefore, in the description of a ''slow'' evolution of the pulse, it is necessary to take into account both the residual dispersion and nonlinearity. Thus rapid breathing oscillations of the pulse are accompanied by slow average changes of the pulse characteristics due to nonlinearity and residual dispersion [19].

In the limit $Z_a, Z_{\mathrm{dis}} \ll Z_{\mathrm{NL}}$, one may treat the nonlinearity as a perturbation. In the lowest order, fast oscillations of the linear pulse amplitude and width are given by

$$A(z,t) = \int_{-\infty}^{+\infty} d\omega A_\omega \exp\left(i\omega t - i\omega^2 \frac{Z_{\mathrm{NL}}}{2Z_{\mathrm{dis}}} \int_0^z d(\xi) d\xi \right). \tag{2}$$

Here A_ω does not depend on z and is determined by initial pulse form. For a Gaussian input signal $A(0,t) = N\exp(-t^2)$ linear oscillations are described by

$$A(z,t) = \frac{N}{\sqrt{\tau(z)}} \exp[-t^2/\tau^2(z) - iCt^2/\tau^2(z) + i\Phi(z)], \tag{3}$$

where $\tau^2(z) = 1 + 16R^2(z), dR(z)/dz = d(z)Z_{\mathrm{NL}}/(2Z_{\mathrm{dis}})$, $C = 4R(z)$, and $\Phi = -0.5\arctan[4R(z)]$. The form of linear solution described above gives hints to the explanation of the Gaussian shape of the asymptotic soliton observed in [23]. Pulse chirping creates an effective parabolic potential that is responsible for the formation of the Gaussian wings in both the linear and nonlinear problems. Nonlinear effects come into play on a large scale compared to Z_a, namely, on the distances proportional to Z_{NL}. Therefore, we use the solution of the linear problem presented above as the starting point for consideration of the nonlinear problem. Recall that the guiding-center soliton concept introduced in [9,6] corresponds to the limit $Z_a \ll Z_{\mathrm{NL}} \sim Z_{\mathrm{dis}}$. We analyze in this work a regime with $Z_{\mathrm{NL}} \gg Z_a \sim Z_{\mathrm{dis}}$ [19]. The existence of the small parameters $Z_{\mathrm{dis}}/Z_{\mathrm{RD}}$ and Z_a/Z_{NL} allows us to introduce fast and slow scales of the evolution [19]. The fast process corresponds to the oscillations of the amplitude and the shape of the pulse; the slow dynamics describes the average changes due to nonlinear effects and residual dispersion. We demonstrate that this slow average dynamics leads asymptotically to the formation of stable breathing structures predicted in [19].

In what follows we adopt the variational approach and derive by means of this method a simple model describing both rapid oscillations and the average pulse evolution under the combined effects of nonlinearity and residual dispersion. Equation (1) can be rewritten after a trivial transformation ($A = Q(t,z)\exp[\int_0^z G(z')dz']$) in the Lagrangian form

$$S = \int L\, dt\, dz = \int dt\, dz \left[\frac{i}{2}(QQ_z^* - Q^*Q_z) + \frac{Z_{\mathrm{NL}}}{2Z_{\mathrm{dis}}} d(z)|Q_t|^2 - \frac{c(z)}{2}|Q|^4 \right]. \tag{4}$$

Here $c(z) \equiv \exp[2\int_0^z G(z')dz']$ can be presented as a sum of rapidly varying and constant parts $c(z) = \langle c(z)\rangle + \tilde{c}(z)$, where $\langle \tilde{c}(z)\rangle = 0$ and $\langle c(z)\rangle = \langle \exp[2\int_0^z G(z')dz']\rangle = [1-\exp(-2\gamma z_a)]/2\gamma z_a$. We write also $d(z)$ in the similar form $d(z) = \langle d(z)\rangle + \tilde{d}(z)$, where $\langle \tilde{d}(z)\rangle = 0$ and $\langle d\rangle = [d_- z_c + d_+(z_a - z_c)]/z_a$ is a small perturbation due to an average residual dispersion ($\langle d\rangle \approx Z_{\mathrm{dis}}/Z_{\mathrm{RD}} \ll 1$). Here we use the notation $\langle f\rangle = (1/z_a)\int_0^{z_a} f(z)dz$.

Any solution of Eq. (1) corresponds to an extremum of S. Therefore, to obtain an approximate model describing the pulse evolution in Eq. (1) one can specify some expected general features of a solution in the trial function and obtain a reduced variational problem after integration in t [36,37]. In recent papers [28,21] this approach has been applied to the problem of optical pulse propagation in systems with dispersion compensation. The accuracy of this method depends on the successful choice of a trial function and must be verified by direct numerical integration.

Because nonlinearity and residual dispersion act as small perturbations to the linear dynamics, we assume that an asymptotic pulse structure will be close to the one given by Eq. (3). Therefore, to describe both rapid pulse width oscillations and slow dynamics due to nonlinearity and residual dispersion let us choose a trial function in the form

$$Q(z,t) = a(z) f[t/b(z)] \exp[i\lambda(z) + i\mu(z)t^2]. \tag{5}$$

Inserting the trial function given by Eq. (5) into Eq. (4), we obtain the reduced variational problem with

$$\langle S\rangle = \int \langle L\rangle dz, \tag{6}$$

$$\langle L\rangle = a^2 b \int |f(s)|^2 ds \lambda_z + a^2 b^3 \int s^2 |f(s)|^2 ds \mu_z + \frac{Z_{\mathrm{NL}}}{2Z_{\mathrm{dis}}} d(z) \left[a^2 b^{-1} \int |f_s|^2 ds + 4\mu^2 a^2 b^3 \int s^2 |f(s)|^2 ds \right] - \frac{c(z)}{2} a^4 b \int |f(s)|^4 ds. \tag{7}$$

After simple calculations one can derive equations describing the evolution of the parameters $a(z)$, $b(z)$, and $\mu(z)$ (see, e.g., [36,37]),

$$a^2 b = \mathrm{const} = N^2, \tag{8}$$

$$b_z = \frac{2Z_{\mathrm{NL}} d(z)}{Z_{\mathrm{dis}}} b\mu, \tag{9}$$

$$\mu_z + \frac{2Z_{\mathrm{NL}} d(z)}{Z_{\mathrm{dis}}} \mu^2 = \frac{Z_{\mathrm{NL}} d(z) C_1}{2Z_{\mathrm{dis}} b^4} - \frac{c(z) N^2 C_2}{b^3}. \tag{10}$$

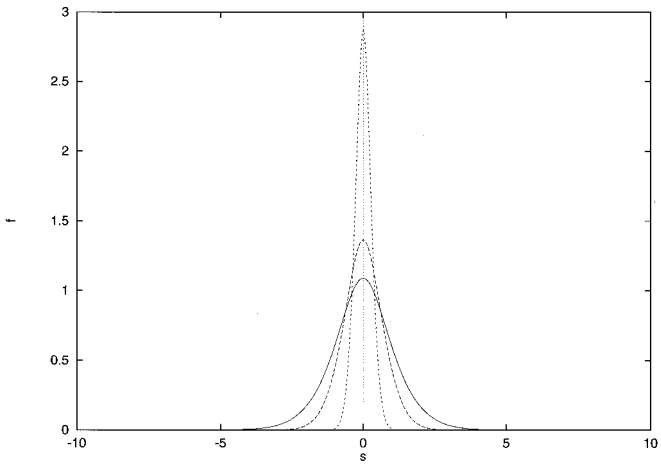

FIG. 2. Localized solutions of Eq. (18) in different limiting cases. Here $\alpha_1=\lambda=0.5$, $\alpha_2=1$, and $\alpha_1 C_1-\alpha_2 C_2=a$. Solid line, solution with $a=0.1$; pulse in the middle, $a=1$; and upper solution, $a=50$.

Here $C_1=\int_{-\infty}^{+\infty}|f_x|^2dx/\int_{-\infty}^{+\infty}x^2|f|^2dx$ and $C_2=\int_{-\infty}^{+\infty}|f|^4dx/4\int_{-\infty}^{+\infty}x^2|f|^2dx$. For instance, for the soliton pulse $f(x)=\mathrm{sech}(x)$, $C_1=2C_2=4/\pi^2$, and for the Gaussian shape $f(x)=\exp(-x^2)$, $C_1=4$ and $C_2=1/\sqrt{2}$. These equations describe the evolution of the pulse parameters under the combined action of fast variations of the dispersion and amplification and the slow dynamics due to nonlinearity and residual dispersion.

Introducing $\nu=\mu b$, we can obtain from Eqs. (9) and (10)

$$\nu_z=\frac{Z_{\mathrm{NL}}d(z)C_1}{2Z_{\mathrm{dis}}b^3}-\frac{c(z)N^2C_2}{b^2}. \tag{11}$$

To describe propagation of the initial pulse in the form $A(0,t)=N\exp(-t^2)$ we fix as initial conditions to Eqs. (9) and (11) $b|_{z=0}=1$, $d\nu/dz|_{z=0}=0$, $C_1=4$, and $C_2=1/\sqrt{2}$. The solution of these equations in the linear case [without the last term in Eq. (11)] has the form $b_l^2=1+16R^2(z)$, where $R(z)$ has been defined above.

In the limit $Z_a, Z_{\mathrm{dis}}\ll Z_{\mathrm{NL}}$, one may again treat the nonlinearity as a perturbation. At the lowest order, fast oscillations of the pulse amplitude and width are given by the solution of the linear problem

$$\frac{d^2B_\pm}{dz^2}=\frac{Z_{\mathrm{NL}}^2d_\pm^2(z)C_1}{Z_{\mathrm{dis}}^2B_\pm^3}. \tag{12}$$

The solution of this equation has the form $B_\pm^2=1+4C_1R_\pm^2(z)$, with $dR_\pm/dz=Z_{\mathrm{NL}}d_\pm/2Z_{\mathrm{dis}}$. This solution describes rapid oscillations due to the variation of dispersion and a slow broadening due to residual dispersion. It follows from here, in particular, that a small change of b over a period due to residual dispersion is given by $b_{\mathrm{res}}=|\langle d(z)\rangle\sqrt{C_1}Z_a/Z_{\mathrm{dis}}|\geqslant 0$.

To obtain the equation governing small changes of $b(z)$ due to nonlinearity we linearize Eqs. (9) and (11) about the linear solution $B_\pm$, assuming $b=B_\pm+\tilde{b}_\pm$ and $\tilde{b}_\pm\ll B_\pm$,

$$\tilde{b}_z=\frac{2Z_{\mathrm{NL}}}{Z_{\mathrm{dis}}}d(z)\tilde{\nu},\quad \tilde{\nu}_z=-\frac{3C_1Z_{\mathrm{NL}}d(z)}{2Z_{\mathrm{dis}}B^4}\tilde{b}-\frac{c(z)N^2C_2}{B^2}. \tag{13}$$

Here and in what follows we drop $\pm$ to avoid complex notation. The initial conditions for Eq. (13) at $z=0$ are $\tilde{b}=0$ and $\tilde{\nu}=0$. The solution of Eq. (13) with these conditions is found as

$$\tilde{b}_-=-\frac{2Z_{\mathrm{NL}}d_-N^2C_2B_z}{Z_{\mathrm{dis}}}\int_0^z\frac{dy}{B_y^2}\int_0^y\frac{c(x)B_x}{B^2}dx, \tag{14}$$

$$\tilde{b}_+=r_1B_z+r_2B_z\int_{z_c}^z\frac{dy}{B_y^2}-\frac{2Z_{\mathrm{NL}}d_+N^2C_2B_z}{Z_{\mathrm{dis}}}\int_{z_c}^z\frac{dy}{B_y^2}\int_{z_c}^y\frac{c(x)B_x}{B^2}dx. \tag{15}$$

The coefficients r_1 and r_2 are determined by matching these solutions at $z=z_c$. The resulting change of the pulse width due to nonlinearity over one period in the main order is given by

$$\tilde{b}_+(z_a)=\frac{2N^2C_2Z_{\mathrm{NL}}}{Z_{\mathrm{dis}}}\left[d_-\int_0^{z_c}\frac{c(z)z}{B_-^3}dz-d_+\int_{z_c}^{z_a}\frac{c(z)(z_a-z)}{B_+^3}dz\right]. \tag{16}$$

In the case we consider here $d_-<0$, $d_+>0$, and, respectively, $b_+(z_a)<0$. One can see that under certain conditions the compression of a pulse [$b_+(z_a)<0$] due to nonlinear effects can balance dispersive broadening of a pulse due to residual dispersion ($b_{\mathrm{res}}>0$) even on the one period. A more general situation, however, is when this delicate balance between nonlinear effects and residual dispersion leads to the long-wavelength oscillations that will be described in Sec. III.

The above description is valid for any localized structural function f used in Eq. (5). Now we address the problem of the shape of a breathing soliton. As it has been discovered in [23], the profile of the asymptotic pulse is very close to the Gaussian shape. This corresponds to the quasilinear solution given by Eq. (3), as mentioned above. On the other hand, as was found in [19] in some particular limits, a breathing soliton is described again by the NLS equation and the asymptotic pulse profile is close to sech. Now we use the same variational principle to analyze the general features of the function f. Assume that the asymptotic pulse presents an oscillating quasisoliton. More concretely, we suppose that the shape of the pulse is reproduced after passing the compensating cell. This assumption is based on the results of numerical simulations of [23,22] and numerical results presented below. In terms of the developed variational approach this means that there are periodic solutions $b(z)$ and $\mu(z)$ of Eqs. (9) and (10). Using the results obtained above and this assumption, let us choose a trial function in the form

$$Q(z,t)=\frac{N}{\sqrt{b(z)}}f[t/b(z)]\exp[i\lambda z+i\mu(z)t^2], \tag{17}$$

where $b(z)$ and $\mu(z)$ are periodic solutions of Eqs. (9) and (10) with some arbitrary C_1 and C_2 [we start here from arbitrary C_1, C_2 and find the corresponding $f(s)$]. Because any solution of Eq. (1) must realize the extremum of the action S, we can consider now the variational problem $\delta S=0$ as a way to determine general features of the structural function f. Averaging the Lagrangian over a period in z yields, after simple calculations, the equation of the shape of the asymptotic pulse $f(s)$,

$$\alpha_1 \frac{d^2 f}{ds^2} + \alpha_2 |f|^2 f - \lambda f - (\alpha_1 C_1 - \alpha_2 C_2) s^2 f = 0, \quad (18)$$

where $\alpha_1 = Z_{\mathrm{NL}}/2Z_{\mathrm{dis}}\langle d(z)/b^2\rangle$, $\alpha_2 = N^2\langle c(z)/b\rangle$, and the angular brackets denote averaging over one period in z. The pulse shape in two important limits can be found from Eq. (18). In the quasilinear case $\alpha_2 \to 0$, the solution is evidently close to the pure Gaussian shape. When $\alpha_1 C_1 = \alpha_2 C_2$, the pulse profile is close to the fundamental soliton of the NLS equation (NLSE). In the general case the localized solution presents some intermediate state between the fundamental soliton and the Gaussian shape. Solutions of Eq. (18) for different limiting cases are shown in Fig. 2. To illustrate different cases, we set $\alpha_1 = \lambda = 0.5$, $\alpha_2 = 1$, and $\alpha_1 C_1 - \alpha_2 C_2 = a$. The solution with $a = 0.1$ (close to the NLSE soliton) is shown by the solid line, the pulse in the middle corresponds to $a = 1$, and the narrow upper solution is for $a = 50$. For not small a the solution can be approximated with good accuracy by the Gaussian distribution. A general feature of the structural function f is that it has the Gaussian wings in the typical case. The Gaussian-like shape of the pulse results from the effective parabolic potential that occurs due to the pulse chirping ($\alpha_1 > 0$). Another conclusion from Eq. (18) is that a localized asymptotic pulse can be formed in the case of the anomalous path average dispersion. Thus this simple qualitative approach explains some observations of [23]. More details on the comparison of this solution with numerical simulations of [23] will be discussed elsewhere.

Equations (9) and (11) give an approximate description of the breathing dynamics of optical pulses in cascaded optical systems with dispersion compensation. As was shown in [38], the variational approach in the nondissipative NLSE is not applicable to the description of the quantitative interaction of the soliton with radiation. Therefore, one should be very careful in making quantitative conclusions about the soliton interaction with radiation from the method developed above. It should be combined with direct numerical simulations. We note that for distances of tens amplifications periods (this case is of importance for European fiber links, for instance), this approximate description of the pulse evolution is in good agreement with the results of numerical simulations [22]. As will be shown below, however, the variational approach with the simple trial function in the form (5) does not always keep the important features of the solution of Eq. (1) that appear on large scales.

III. AVERAGED DYNAMICS

In this section we present the averaged equations describing, in the main order, a slow pulse evolution due to nonlinearity and residual dispersion. To describe fast pulse width oscillations let us make the Fourier transformation $Q(z,t) = (1/\sqrt{2\pi}) \int d\omega Q_\omega \exp(-i\omega t)$. The action S is transformed to

$$S = \int L\, dt\, dz = \int dz\, d\omega \left[\frac{i}{2}(Q_\omega Q^*_{\omega z} - Q^*_\omega Q_{\omega z}) + \frac{Z_{\mathrm{NL}}}{2Z_{\mathrm{dis}}} d(z) \omega^2 |Q_\omega|^2 - \frac{c(z)}{4\pi} \int d\omega_1 d\omega_2 Q_\omega Q^*_{\omega_1} Q^*_{\omega_2} Q_{\omega_1+\omega_2-\omega} \right]. \quad (19)$$

As was mentioned above, in the limit $Z_a, Z_{\mathrm{dis}} \ll Z_{\mathrm{NL}}$, one may treat the nonlinearity as a perturbation. In the lowest order, fast oscillations of the pulse width are given by Eq. (2). The fast process corresponds to the oscillations of the amplitude and the shape of the pulse due to periodic amplification and dispersion compensation and the slow evolution is due the average changes due to nonlinear effects and residual dispersion. Therefore, we assume that Q_ω varies slowly with z and present $Q(t,z)$ in the form

$$Q(t,z) = \int_{-\infty}^{+\infty} d\omega\, \Psi(\omega,z) \exp[i\omega t - i\omega^2 R(z)]. \quad (20)$$

Here $dR/dz = (Z_{\mathrm{NL}}/2Z_{\mathrm{dis}}) d(z)$. Note that in the limit $Z_{\mathrm{dis}} \ll Z_a \ll Z_{\mathrm{NL}}$ from Eq. (20) a general structure of the asymptotic form of a breathing pulse can be obtained. Indeed, in this limit $R \sim Z_a/Z_{\mathrm{dis}} \gg 1$ and the integral (20) can be approximated using the method of stationary phase. This yields (omitting insignificant multipliers)

$$A(z,t) = \exp\left(\int_0^z G(z')dz' \int_{-\infty}^{+\infty} d\omega\, \Psi_\omega(z) \times \exp[i\omega t - i\omega^2 R(z)] \right) \sim \frac{\exp\left(\int_0^z G(z')dz' \right)}{\sqrt{R(z)}} \Psi\left(\frac{t}{2R(z)} \right) \exp\left(-i \frac{t^2}{4R(z)} \right). \quad (21)$$

Note that this asymptotic form of the breathing soliton has the same structure as the solution of the linear problem (3) in the case of large R. The difference is that the shape of the soliton or the structural function Ψ is determined by the interplay between residual dispersion and nonlinearity.

To obtain the equation for the slow average evolution of $Q(t,z)$ we substitute Eq. (20) into the Lagrangian and average L over the interval Z_a. Because the function $\Psi(\omega,z)$ is assumed to vary slowly on the amplification distance, it can be placed outside the averaging integral. After straightforward calculations we obtain the Lagrangian describing the evolution of the slowly varying envelope.

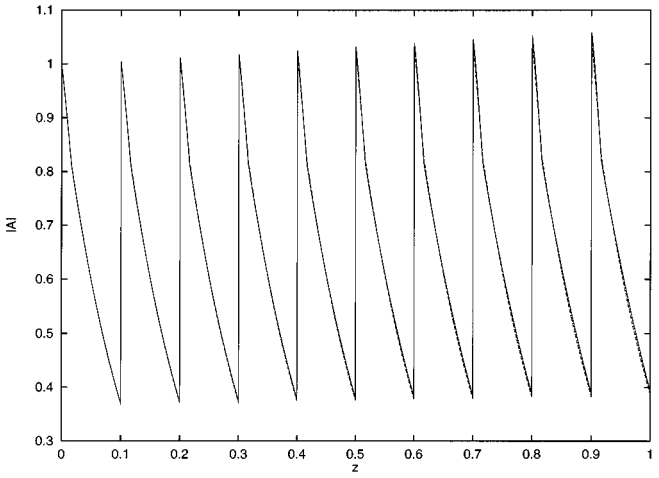

FIG. 3. Comparison of the variational approach and direct numerical simulations. Dashed line, oscillations of the $|A|$ obtained by means of the variational approach; solid line, direct simulations of Eq. (1). The input pulse is of the form $A(t,0)=\exp(-t^2/4)$, $\langle d\rangle=0.05$.

$$S_{\rm av}=\int \widetilde{L}\,dt\,dz=\int dz\,d\omega\left[\frac{i}{2}[\Psi(\omega)\Psi_z^*(\omega)-\Psi^*(\omega)\Psi_z(\omega)]+\frac{Z_{\rm NL}}{2Z_{\rm dis}}d(z)\omega^2|\Psi_\omega|^2\right]-\int dz\,d\omega_1 d\omega_2 d\omega_3 d\omega_4 \Psi_{\omega_1}\Psi_{\omega_2}\Psi^*_{\omega_3}\Psi^*_{\omega_4}\times\delta(\omega_1+\omega_2-\omega_3-\omega_4)F(\omega_1,\omega_2,\omega_3,\omega_4), \quad (22)$$

where the function F is given by

$$F=\frac{1}{4\pi Z_a}\left\{\frac{1-\exp[-2\gamma Z_c(1+igd_-)]}{2\gamma(1+igd_-)}+\frac{\exp[-2\gamma Z_c-i2\gamma g d_+(Z_c-Z_a)]-\exp(-2\gamma Z_a)}{2\gamma(1+igd_+)}\right\}. \quad (23)$$

Here $g=(\omega_1^2+\omega_2^2-\omega_3^2-\omega_4^2)/4\gamma Z_{\rm dis}$. Thus the equation describing the slow evolution of $\Psi(\omega,z)$ reads

$$i\frac{\partial\Psi_\omega(z)}{\partial z}-\omega^2\frac{Z_{\rm NL}}{2Z_{\rm dis}}\langle d(z)\rangle\Psi_\omega(z)+2\int_{-\infty}^{+\infty}d\omega_1 d\omega_2 d\omega_3\times\delta(\omega_1+\omega_2-\omega-\omega_3)F(\omega_1,\omega_2,\omega_3,\omega)\Psi_{\omega_1}\Psi_{\omega_2}\Psi^*_{\omega_3}. \quad (24)$$

Equation (24) can be written in the Hamiltonian form

$$i\frac{\partial\Psi_\omega(z)}{\partial z}=\frac{\delta H}{\delta\Psi_{\omega^*}}, \quad (25)$$

with the Hamiltonian

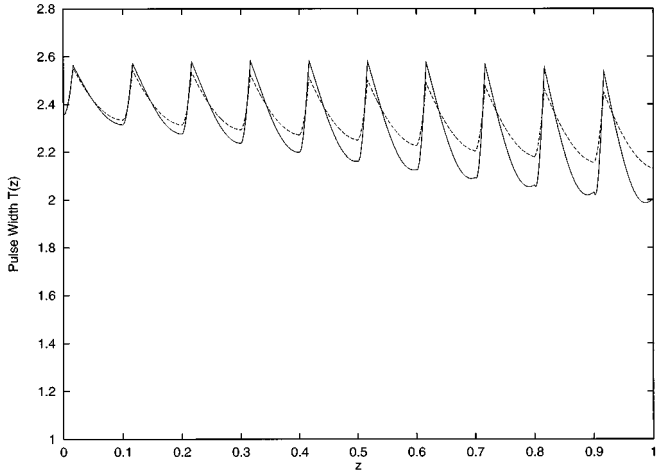

FIG. 4. Same as in Fig. 3, but for the pulse width (FWHM) $T(z)$. Dashed line, oscillations of the $T(z)$ obtained by the variational approach; solid line, direct simulations of Eq. (1).

$$H=\frac{Z_{\rm NL}}{2Z_{\rm dis}}\langle d(z)\rangle\int\omega^2|\Psi_\omega|^2d\omega-\int_{-\infty}^{+\infty}d\omega_1 d\omega_2 d\omega_3 d\omega_4\delta(\omega_1+\omega_2-\omega_3-\omega_4)\times F(\omega_1,\omega_2,\omega_3,\omega_4)\Psi_{\omega_1}\Psi_{\omega_2}\Psi^*_{\omega_3}. \quad (26)$$

Of course, the Hamiltonian H is real because $F^*(g)=F(-g)$. For instance, for the case of lossless fiber ($\gamma=0$) and equal lengths of DCF and SMF pieces ($d_-=-d_+$), it can be found that

$$F(\omega_1,\omega_2,\omega_3,\omega)=\exp(i\Phi)\sin(\Phi)/4\pi\Phi,$$

where

$$\Phi=(\omega_1^2+\omega_2^2-\omega_3^2-\omega^2)Z_a d_+/8Z_{\rm dis}.$$

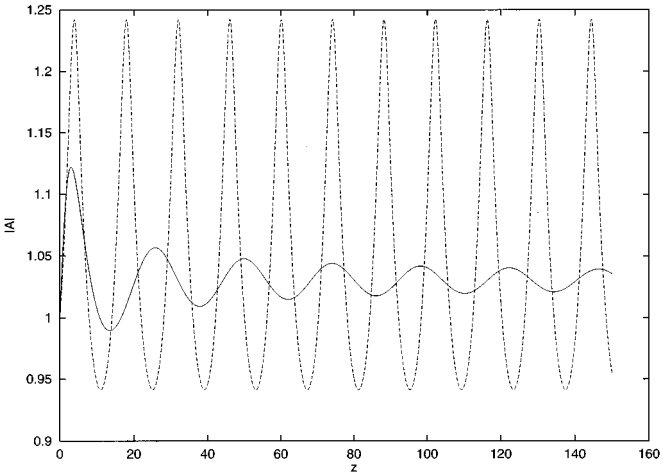

FIG. 5. Comparison of the direct simulations and variational description in the long-term pulse evolution. The pulse amplitude at the amplifiers ($z_k=z_a k=0.1k$ with $k=1,2,\ldots$) is plotted with the same initial conditions as in Figs. 3 and 4.

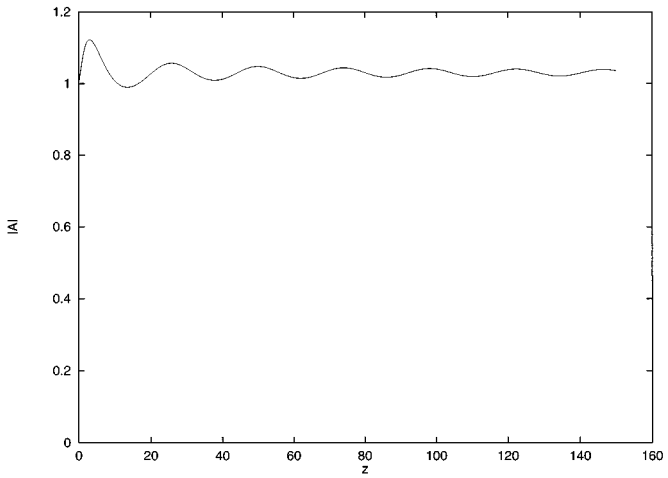

FIG. 6. Long-term evolution of the envelope of the pulse amplitude over many amplification periods. The envelope is shown at points of the amplifiers location. The initial conditions are $A(0,t)=N/\cosh(t)$, $N^2=2\gamma Z_a/[1-\exp(-2\gamma Z_a)]$, and $\langle d\rangle=0.05$.

The integral $P=\int|\Psi_\omega|^2 d\omega$ is an additional conserved quantity. The averaged soliton of the form $\Psi(z,\omega)=\Psi_0(\omega)\exp(i\lambda^2 z)$ realizes the extremum of the H for a fixed P,

$$\delta(H+\lambda^2 P)=0. \tag{27}$$

Again it can be shown that localized solutions exist only in the case of the anomalous path average dispersion, i.e., positive $\langle d(z)\rangle$. Note that the dynamics of the localized average pulse depends on the dispersion map. The typical solution presents a central peak interacting with radiation. Radiation can be suppressed by special dispersion mapping [23]. Equation (24) describes the slow averaged evolution of the pulse due to the combined action of nonlinearity and residual dispersion. Results of the numerical simulations demonstrating such an averaged dynamics will be presented in the following section.

IV. ASYMPTOTIC PULSE FORMATION

Here we discuss the results of comparative and asymptotic numerical analyses of a general model given by

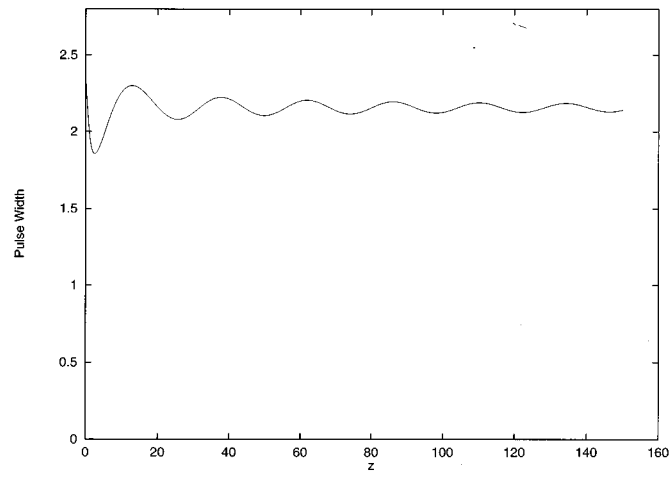

FIG. 7. Same as in Fig. 6, but for the pulse width.

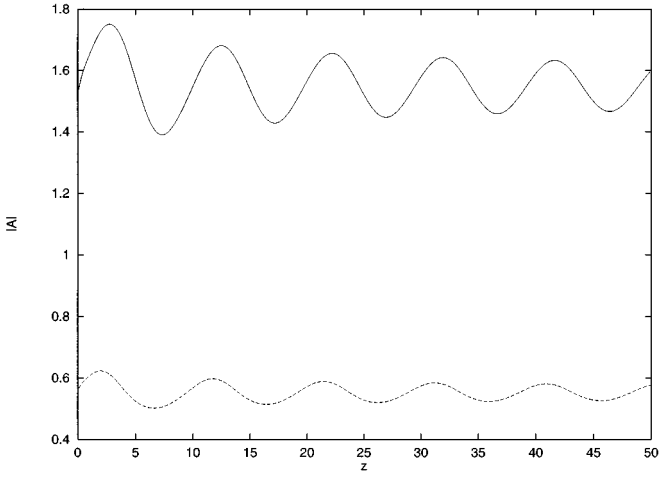

FIG. 8. Variations of the pulse amplitude maxima and minima. The input signal is the same as in Figs. 6 and 7. The upper line is for the maximum of the pulse amplitude on the amplification period and the lower line corresponds to the minimum of the pulse amplitude in the span between two amplifiers.

Eq. (1) and a truncated variational model given by Eqs. (9) and (11). The parameters used in the calculations are $Z_{\rm NL}=360$ km and $Z_a=Z_{\rm dis}=36$ km; which correspond to the input pulse power of the order of several megawatts and $t_0\approx 27$ ps. The dimensionless residual dispersion $\langle d\rangle$ used in the simulations varies from 0.05 to 0.1. The characteristic length of the residual dispersion corresponding to $\langle d\rangle=0.1$ is $Z_{\rm RD}=360$ km. Other parameters are $\alpha=0.25$ dB/km($\gamma=0.115\alpha$); the length of the DCF piece, $Z_c=6$ km; $D_-=-80$ ps/nm km, and $D_+=18$ ps/nm km.

First, we demonstrate that the variational approach in the form presented above gives a reasonable approximation of the optical pulse dynamics in the system under consideration, but only on relatively short distances. Figures 3 and 4 show the pulse evolution obtained by direct numerical simulations of Eq. (1) (solid line) and by means of the variational approach (dashed line). The spatial evolution of the envelopes $[|A(0,z)|]$ is presented in Fig. 3, while Fig. 4 shows the

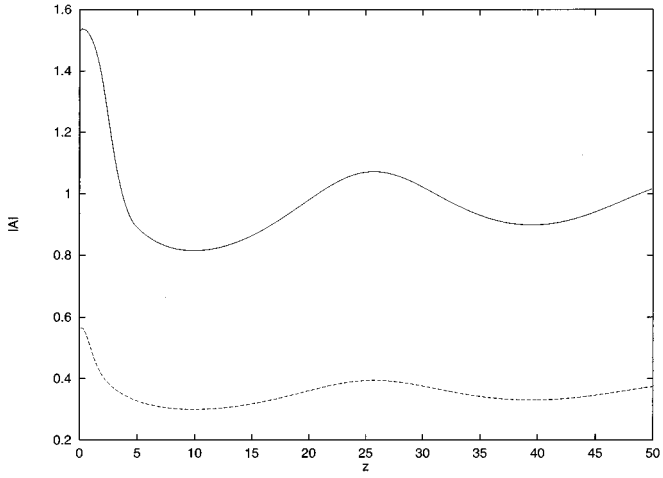

FIG. 9. Averaged dynamics as in Fig. 8, but for the Gaussian input pulse $A(0,t)=1.52\exp(-t^2)$, $\langle d\rangle=0.05$.

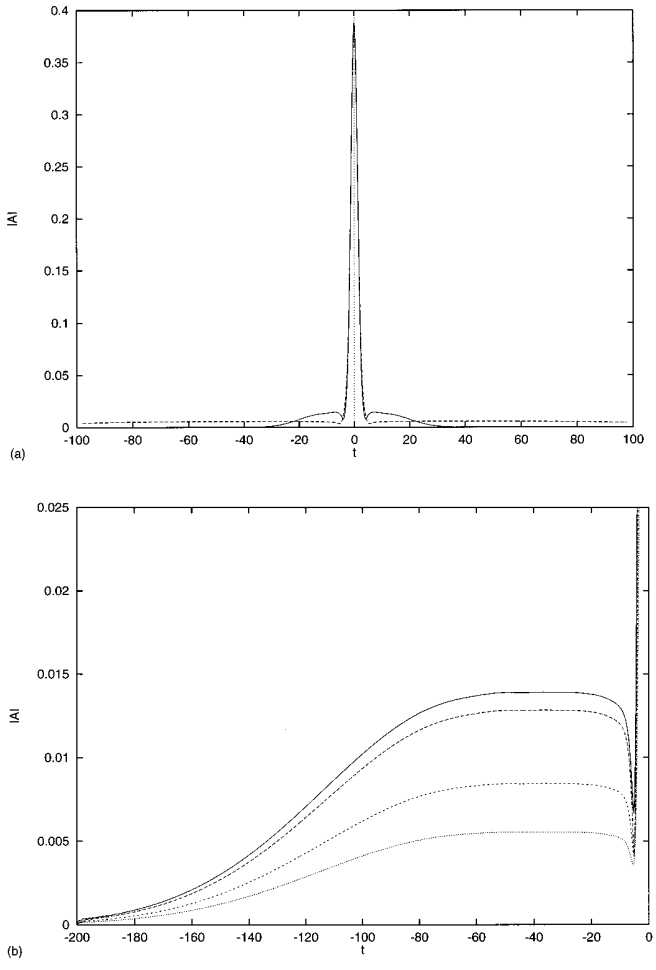

FIG. 10. Structure of the asymptotic state. (a) The shapes of the pulse are plotted for $z=25$ (solid line) and $z=150$ (dashed curve). The initial pulse $A(t,0)=\exp(-t^2/4)$. (b) A closeup view of the tail dynamics.

spatial dependence of the pulse width. The agreement of the direct simulations with the variational approach is very good up to the distance $z\approx 1$, which corresponds to the propagation distance of about 360 km. In Figs. 3 and 4 the fast dynamics of the pulse is shown. Small changes over one period lead to the slow evolution of the pulse parameters. To describe the slow evolution, we will use the following pulse characteristics: the maximum and minimum of the pulse amplitude and width on the amplification period and the pulse width and amplitude at the amplifiers (located at $z_k=z_a k$, with $k=1,2,3,\ldots$). The long-term (averaged) pulse evolution is shown in Fig. 5. In Fig. 5 the pulse amplitude at the amplifiers found by means of the variational approach (dashed line) and by means of direct simulations of Eq. (1) (solid line) is plotted. As follows from Fig. 5, at larger distances the results of the simulations diverge considerably and truncated variational model with the trial function in the form (5), which keeps the main rough features of the dynamics, is not valid for the quantitative description of the pulse propagation.

Due to the quasilinear character of the rapid oscillations, the general features of the dynamics do not depend significantly on the particular shape of the input signal. On the scale of many amplification distances, the input pulse

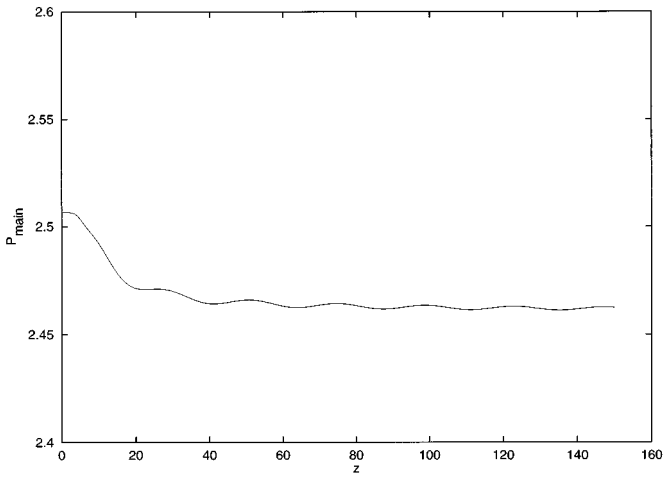

FIG. 11. Evolution of the pulse energy defined as $P_{\rm main}=\int_{-5}^{5}|A|^2dt$. The initial conditions are the same as in Fig. 10. $P_{\rm main}$ versus z is plotted.

evolves into a new state that manifests itself as a breathing solitary wave. The speed and features of this transition depend on the residual dispersion value, input pulse parameters, and its shape. Figures 6–8 demonstrate the oscillating structure that emerges from the initial pulse $A(0,t)=N/\cosh(t)$. In Figs. 6 and 7 the pulse amplitude and width, respectively, at the amplifiers are shown. Note that the amplification distance $z_a=0.1$ in the dimensionless variables; therefore, this figure can be considered as an average description of the pulse dynamics. The fast breathing dynamics is accompanied by slow average oscillations due to nonlinearity and residual dispersion. In the asymptotic state the amplitude of these oscillations is smaller than during the transition period. However, we did not find in our numerical simulations a state for which such slow oscillations are absent. Figures 8 and 9 illustrate how the asymptotic state can depend on the input pulse shape. In these figures the upper line is for the maximum of the pulse amplitude on the amplification period and the lower line corresponds to the averaged minimum of the pulse amplitude. Figure 9 shows that for the initial Gaussian pulse, on average, oscillations are smaller and have a larger period in comparison to the sech input pulse (Fig. 8). It should be pointed out that quasistable propagation is possible if a residual dispersion coefficient $D_{\rm res}$ is positive (anomalous dispersion region). Only in this case is the propagation of breathing bright soliton possible, even in the presence of DCF pieces with high normal dispersion. If the residual dispersion is negative, dark solitons can propagate in such a system. We use here the term breathing soliton, though the shape of the final state is not sech, as for guiding-center solitons. As was shown in [23], an asymptotic pulse forming after many amplification periods is closer to the Gaussian profile rather than to sech.

The asymptotic state that is formed with a pulse propagation along the system is not stationary even in the averaged description. The pulse structure, as can be clearly seen from Fig. 10(a), consists of the main peak interacting with tail of continuous radiation. The shapes of the pulse are presented for the different values of $z=25$ and $z=150$. The simulations have been performed for the initial pulse $A(t,0)=\exp(-t^2/4)$. Integration has been performed from

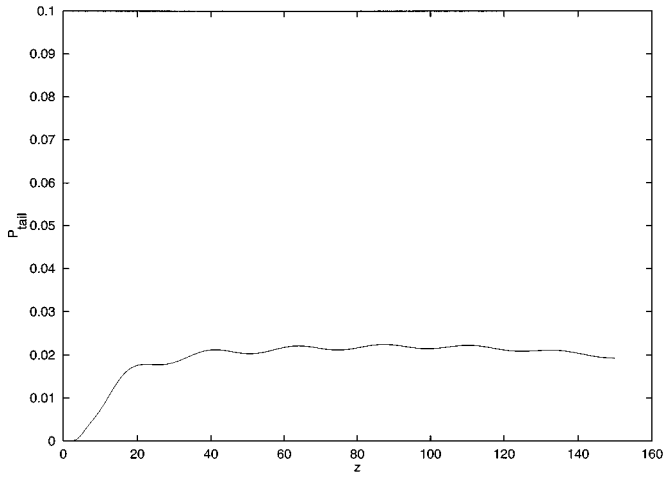

FIG. 12. Same as in Fig. 11, but for the tail energy defined as $P_{\rm tail}=\int_{-200}^{200}|A|^2dt$. $P_{\rm tail}$ versus z is plotted.

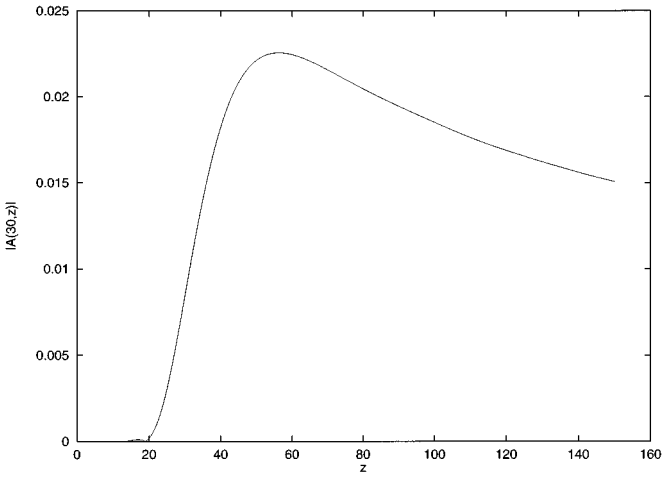

FIG. 13. Evolution of the tail amplitude. The function $|A(30,z)|$ is plotted as a function of z.

-200 to 200 in t to avoid the influence of the boundary effects on the tail evolution. The central part of the peak is close to a Gaussian distribution in accordance with the results of [23]. Figure 10(b) presents a closeup view of the tail dynamics. This figure demonstrates that the pulse propagating down the fiber link emits radiation that spreads due to dispersion. Figures 11 and 12 show the evolution of the pulse and the tail energies, respectively. In many ways the asymptotic pulse dynamics of our model is similar to asymptotic solutions of the NLS equation studied in [38]. This dynamics has two basic stages, namely, the ''fast'' separation of radiative part from the initial pulse and the ''slow'' interaction of continuous radiation with the main pulse. In our particular case the process of radiative tail separation is completed at the distance $z\approx 20$ (see Figs. 12 and 13) for the chosen initial field distribution. The amount of energy of continuous radiation is less than 1% of the energy of the main pulse. The further interaction of continuous radiation with the main pulse has the character of decreasing oscillations. The corresponding energies of the radiative tail and the main pulse are approaching their constant values. This behavior is in good qualitative agreement with the pulse dynamics in the integrable NLS equation described in [38]. The period of oscillations is approximately equal to 25.5 (the dispersion length in our case is equal to 0.1).

Continuous radiation leads to the bit rate limitation in fiber optical links. The source of these limitations is the nonlocal character of the pulse interactions in the bit stream through continuous radiation. The description of a such an interaction will be presented in a separate paper.

V. CONCLUSIONS

In conclusion, we have studied numerically and by means of the variational approach an asymptotic breathing optical pulse propagating through cascaded transmission systems with periodic amplification and dispersion compensation. We have derived approximate equations describing the pulse amplitude and width oscillations and found that results obtained by this approach are in good agreement with the results of direct numerical modeling on the short and middle distances. This approximate variational approach explains two important observations of the numerical work [23]: the Gaussian shape of the asymptotic pulse and the formation of a quasistable pulse only in the case of anomalous path average dispersion. We have found that an input pulse evolves asymptotically into a stable breathing structure. After the first stage of propagation, the input pulse emits radiation that spreads due to dispersion. The asymptotic structure that is formed realizes a balance between the main pulse and the radiative tail. The results of our numerical simulations confirm the possibility of ''breathing'' pulse transmission.

ACKNOWLEDGMENTS

We would like to thank A. Mattheus for helpful discussion. This research has been supported in part by RFBR Grant Nos. 96-02-19131 and 96-02-19129. The support of EEC in the framework of ACTS Project UPGRADE is acknowledged.

[1] Neal S. Bergano, C. D. Davidson, D. L. Wilson, F. W. Kerfoot, M. D. Tremblay, M. D. Levanas, J. P. Morreale, J. D. Erankow, P. C. Corbett, M. A. Mills, G. A. Ferguson, A. M. Vengsarkar, J. R. Pedrazzani, J. A. Nagel, J. L. Zyskin, and J. W. Sulhoff, in *Proceedings of the Optical Fiber Communication Conference, San Jose, 1996*, Vol. 2 of 1996 OSA Technical Digest Series (Optical Society of America, Washington, 1996), Postdeadline paper PD23-1, p. 12.

[2] L. F. Mollenauer, P. V. Mamyshev, and M. J. Neubert Electron. Lett. **32**, 471 (1996).

[3] T. Morioka, H. Takara, S. Kawanishi, O. Kamatani, K. Takaguchi, K. Uchiyama, M. Saruwatari, H. Takahashi, M. Yamada, T. Kanamori, and H. Ono, in *Proceedings of the Optical Fiber Communication Conference, San Jose, 1996* (Ref. [1]),

Postdeadline paper PD21-1, p.11.
[4] A. H. Gnauck, A. R. Chraplyvy, R. W. Tkach, J. L. Zyskind, J. W. Sulhoff, A. J. Lucero, Y. Sun, R. M. Jopson, F. Forghieri, R. M. Derosier, C. Wolf, and A. R. McCormick, in *Proceedings of the Optical Fiber Communication Conference, San Jose, 1996* (Ref. [1]), Postdeadline paper PD20-1, p. 23.
[5] H. Onaka, H. Miyata, G. Ishikawa, K. Otsuka, H. Ooi, Y. Kai, S. Kinoshita, M. Seino, H. Nishimoto, and T. Chikama; Electron. Lett. **31**, 1461 (1995).
[6] L. F. Mollenauer, S. G. Evangelides, Jr., and H. A. Haus, IEEE J. Lightwave Tech. **9**, 194 (1994).
[7] M. Nakazawa and H. Kubota, Electron. Lett. **31**, 216 (1995).
[8] L. F. Mollenauer, P. V. Mamyushev, and M. J. Neubelt, Opt. Lett. **19**, 704 (1995).
[9] A. Hasegawa and Y. Kodama, Opt. Lett. **15**, 1444 (1990); Phys. Rev. Lett. **66**, 161 (1991).
[10] K. J. Blow and N. J. Doran, IEEE Photon. Technol. Lett. **3**, 369 (1991).
[11] A. Mattheus and S. K. Turitsyn, in *Proceedings of the 20th European Conference on Optics Communications, Montreux, 1993* (Drucerei Richterswil AG, Richterswil, 1993), Vol. 2, p. 37.
[12] F. M. Knox, W. Forysiak, and N. J. Doran, IEEE J. Lightwave Tech. **13**, 1955 (1995).
[13] R. Kashyap, Opt. Fiber Tech. **1**, 17 (1994).
[14] C. Lin, H. Kogelnik, and L. G. Cohen, Opt. Lett. **5**, 476 (1980).
[15] H. Onaka, H. Miyta, K. Otsuka, and T. Chikama, in *Proceedings of the 20th European Conference on Optics Communications, Florence, 1994* (Instituto Internazionale delle Communicazioni, Genova, 1994), Vol. 4, p. 49.
[16] A. D. Ellis and D. M. Spirit, Electron. Lett. **30**, 72 (1994).
[17] S. Artigaud, M. Chbat, P. Nouchi, F. Chiquet, D. Bayart, L. Hamon, A. Pitel, F. Goudeseune, P. Bousselet, and J-L. Beylat, Electron. Lett., **32**, 1389 (1996).
[18] C. Das, U. Gaubatz, E. Gottwald, K. Kotten, F. Küppers, A. Mattheus, and C. J. Weiske, Electron. Lett. **31**, 305 (1995).
[19] I. Gabitov and S. K. Turitsyn, Opt. Lett. **21**, 327 (1996); Los Alamos Report No. LAUR-95-3633, 1995 (unpublished).
[20] I. Gabitov, F. Küppers, A. Mattheus, and S. Turitsyn, Los Alamos Report No. LAUR-95-2230, 1995 (unpublished).
[21] I. Gabitov and S. K. Turitsyn, Pis'ma Zh. Eksp. Teor. Fiz. **63**, 814 (1996) [JETP Lett. **63**, 862 (1996)].
[22] I. Gabitov, E. G. Shapiro, and S. Turitsyn, Opt. Commun. **134**, 317 (1996).
[23] N. Smith, F. M. Knox, N. J. Doran, K. J. Blow, and X. Bennion, Electron. Lett. **32**, 55 (1995).
[24] N. Smith and N. J. Doran, Opt. Lett. **21** , 570 (1996).
[25] D. Breuer and K. Petermann, AEU Int. J. Electron. Commun. **50**, 310 (1996).
[26] M. Nakazawa and H. Kubota, Jpn. J. Appl. Phys. **34**, L681 (1995).
[27] F. Küppers, A. Mattheus, and R. Ries, Pure Appl. Opt. **4**, 459 (1995).
[28] A. Berntson, D. Anderson, M. Lisak, M. L. Quiroga-Teixeiro, and M. Karlsson, Opt. Commun. **130**, 153 (1996).
[29] F. M. Knox, P. Harper, P. N. Kean, I. Bennion, and N. J. Doran, in *Proceedings of the 22nd European Conference on Optics Communications, Oslo, 1996* (Telenor R&D, Kjeller, Norway, 1996), Vol. 3, p. 101.
[30] J. M. Jacob, E. A. Golovchenko, A. N. Pilipetskii, G. M. Carter, and C. R. Menyuk, IEEE Photon. Tech. Lett. **9**, 130 (1997).
[31] J. C. Bronski and J. N. Kutz, Opt. Lett. **21**, 937 (1996).
[32] F. Kh. Abdullaev, S. A. Darmanyan, A. Kobyakov, and F. Lederer, Phys. Lett. A **220**, 213 (1996).
[33] B. Malomed, D. Parker, and N. Smyth, Phys. Rev. E **48**, 1418 (1993).
[34] R. Grimshaw, J. He, and B. Malomed, Phys. Scr. **53**, 385 (1996).
[35] G. P. Agrawal, *Nonlinear Fiber Optics* (Academic, San Diego, 1989).
[36] D. Anderson, Phys. Rev. A **27**, 3135 (1983); D. Anderson and M. Lisak, Opt. Lett. **10**, 390 (1985).
[37] D. Anderson and M. Lisak, Opt. Lett. **10**, 134 (1985); D. Anderson, M. Lisak, B. Malomed, and M. Quiroga-Teixeiro, J. Opt. Soc. Am. B **11**, 2380 (1994); B. Malomed, Opt. Lett. **19**, 341 (1994); D. Anderson, M. Lisak, and T. Reichel, J. Opt. Soc. Am. B**5**, 207 (1988).
[38] E. A. Kuznetsov, A. V. Mikhailov, and I. A. Shimokhin, Physica D **87**, 201 (1995).